

Data processing and initial results of Chang'e-3 lunar penetrating radar *

Yan Su¹, Guang-You Fang², Jian-Qing Feng¹, Shu-Guo Xing¹, Yi-Cai Ji², Bin Zhou²,
Yun-Ze Gao², Han Li¹, Shun Dai¹, Yuan Xiao¹ and Chun-Lai Li¹

¹ Key Laboratory of Lunar and Deep Space Exploration, National Astronomical Observatories,
Chinese Academy of Sciences, Beijing 100012, China; suyan@nao.cas.cn

² Institute of Electronics, Chinese Academy of Sciences, Beijing 100190, China

Received 2014 July 21; accepted 2014 September 13

Abstract To improve our understanding of the formation and evolution of the Moon, one of the payloads onboard the Chang'e-3 (CE-3) rover is Lunar Penetrating Radar (LPR). This investigation is the first attempt to explore the lunar subsurface structure by using ground penetrating radar with high resolution. We have probed the subsurface to a depth of several hundred meters using LPR. In-orbit testing, data processing and the preliminary results are presented. These observations have revealed the configuration of regolith where the thickness of regolith varies from about 4 m to 6 m. In addition, one layer of lunar rock, which is about 330 m deep and might have been accumulated during the depositional hiatus of mare basalts, was detected.

Key words: space vehicles: instruments: Lunar Penetrating Radar — techniques: radar astronomy — methods: data processing — Moon: lunar subsurface — Moon: regolith

1 INTRODUCTION

The Moon is the only natural satellite of our Earth. Since the invention of optical telescopes, human beings have been continuously exploring the Moon by different kinds of techniques (Ip et al. 2014). Radar is an attractive and powerful technique to observe the Moon. There are three main goals in using radar to observe the Moon: firstly, to explore the lunar landscape including polar regions; secondly, to probe for water ice at the lunar poles based on high resolution mapping; thirdly, to analyze and study lunar subsurface structures such as the thickness of regolith. The study of subsurface structures is not only useful for better understanding the geologic history of the Moon, but also its thermal history and the origin of the Earth-Moon system (Yamaji 1998).

Radar mapping of the Moon's topography was first done by the Arecibo telescope at a wavelength of 70 cm in 1964 (Thompson & Dyce 1966). Since then, the Goldstone Solar System Radar has been improved to allow 40 MHz bandwidth imaging with Earth based radar interferometric measurements. Images and interferograms with a resolution of about 4 m in range by 5 m in azimuth were subsequently obtained (Hensley et al. 2011). The investigation with Mini-RF consists of polarimetric Synthetic Aperture Radar (SAR) imagers on the ISRO Chandrayaan-1 lunar orbiter and

* Supported by the National Natural Science Foundation of China.

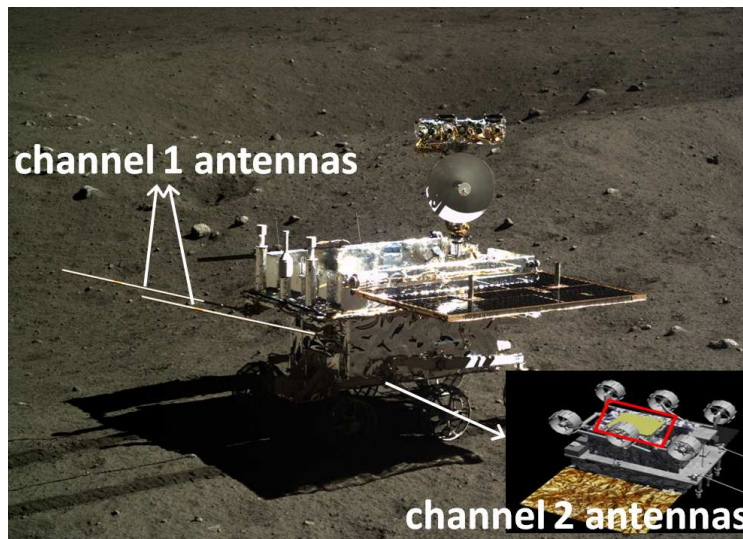


Fig. 1 Illustration of the two radar channels on the LPR. This picture was taken by the descending camera onboard the CE-3 lander when the Yutu rover was on the site denoted by point N0104. One transmitting and one receiving dipole antennas for the first channel of 60 MHz are installed at the back of the Yutu rover. For the second channel that operates at 500 MHz, one transmitting and two receiving bow-tie antennas are attached to the bottom of the Yutu rover.

the NASA Lunar Reconnaissance Orbiter (LRO), which have the primary objective of searching for water ice in permanent shadows at the lunar poles (Kirk et al. 2010; Spudis et al. 2010). Mapping the thickness of the regolith layer on the nearside of the Moon was carried out with Arecibo radar data at a wavelength of 70 cm (Thompson 1987) and distributions of iron and titanium content were derived from Earth-based optical data (Shkuratov et al. 1999). The average thicknesses were found to be 5 m and 12 m respectively for maria and highlands (Shkuratov & Bondarenko 2001). In 1972, the Apollo Lunar Sounder Experiment (ALSE) was the subsurface sounder experiment that flew on the Apollo 17 mission to study the Moon's surface and interior. Its working frequency was 5 MHz, and the estimated depth of penetration was 1.3 km with range resolution of 300 m. The Lunar Radar Sounder (LRS) onboard the Japanese KAGUYA spacecraft (SELENE) found that most nearside maria have subsurface stratifications. The working frequency of LRS is 5 MHz, which enabled subsurface data to be obtained to a depth of several kilometers with a resolution of 75 m (Ono et al. 2010).

Chang'e-3 (CE-3) was launched on 2013 December 2, and it landed successfully on the Moon. The CE-3 rover is called Yutu, and one of the scientific payloads it carries is Lunar Penetrating Radar (LPR). It is the first ground penetrating radar that has operated on the lunar surface. Compared with ALSE and LRS, LPR works at higher frequencies of 60 MHz and 500 MHz (Fang et al. 2014). Thus it can probe regions with shallower depth at higher range resolution. At these two frequencies, it can measure the structure and depth of lunar regolith within 30 m, and investigate the structure of lunar crust to hundreds of meters deep. The LPR transmits nanosecond pulses in the time domain with no carrier frequency. Based on the analysis of radar echo signals, subsurface structures can be revealed. The free space range resolutions are ~ 50 cm and ~ 25 m for 60 MHz and 500 MHz respectively. The LPR uses one transmitting and one receiving dipole antenna for 60 MHz which are installed at the back of the rover. For the 500 MHz system, one transmitting and two bow-tie receiving antennas are attached to the bottom of the rover, as shown in Figure 1.

2 TESTS AND MEASUREMENTS

The landing site of CE-3 is 44.1260N, 19.5014W in Mare Imbrium, about 40 km south of the crater Laplace F. The Yutu rover was successfully deployed from the lander and touched the lunar surface on 2013 December 14. The LPR transmits a pulsed signal and receives the radar echo signal along the path that the Yutu rover traverses. The radar data stop being sampled and are sent back to Earth when Yutu is stationary. Observations are simultaneously carried out at frequencies of 60 MHz and 500 MHz.

Radar data are stored by track. A block of track data contains the relative intensity of the radar echo signal in one time window appended with setting parameters for the instrument. The time window is defined as the length of time for receiving reflected echoes. They are 10 240 ns and 640 ns respectively for the two channels.

During the Yutu rover's traverse, exploration points are designated and set for scientific studies. Also, a number of navigation points are set at short distance steps along the path of the scientific exploration points so that the progress of the Yutu rover can be periodically verified along its route. These points are labeled N0101, N0102, etc.

Figure 2 shows the trajectory of the Yutu rover's traverse. The background image is the topography that was photographed by a descending camera attached to the CE-3 lander while it descended. The LPR started working at 10:50:32 UTC on 2013 Dec. 15. Until 14:16:56 UTC 2014 Jan. 15, LPR had worked for 277 min. 10 171 and 19 934 track data were obtained for the first and second channels respectively. Among these data, 1340 and 2531 track data are valid while the Yutu rover was maneuvering. Others are duplicated and similar when Yutu was stationary.

Two important instrument parameters, i.e. the system gain and cumulative number, need to be tested and confirmed during in-orbit testing of the LPR. In order to expand the dynamic range of the radar system, system gain can be changed with relative amplitude of the radar echo signal. The weaker the relative amplitude of the radar signal is, the greater the system gain should be set. Thus weaker signals could be recognized and LPR would be able to detect deeper subsurface structures. However, further analysis based on relative amplitude of the radar echo signal requires that the relative amplitude of the real original signal must be obtained and the effect of variable gain must be eliminated; this has been done in published data. The cumulative number is the number of radar echo signals accumulated and saved as one block of track data. The smaller the cumulative number is, the greater the radar data volume becomes, which could cause difficulty with downlink transmission of data. When the rover moved from N0101 to N0102, N0103, N0104, N0105 and N0106, different parameter setting were tested in each period to confirm which parameters were optimal, as shown in Table 1.

Figures 3 and 4 are the radar maps at 60 MHz and 500 MHz respectively. They very clearly indicate that the LPR works well and different parameter settings result in different radar maps.

Table 1 Test of Different Parameter Settings for the LPR

Channel No.	Parameter	N0101–N0102	N0102–N0103	N0103–N0104	N0104–N0105	N0105–N0106
Channel 1	Pulse Repetition Frequency (kHz)	1	1	1	1	1
	Cumulative Number	35	35	4	4	4
	Gain Mode	Variable gain	Constant gain	Variable gain	Variable gain	Variable gain
	Attenuation Settings (dB)	31	50	20	10	0
	Valid Data Length	8192	8192	4096	4096	4096
Channel 2	Pulse Repetition Frequency (kHz)	10	10	10	10	10
	Cumulative Number	18	18	15	15	15
	Gain Mode	Variable gain	Constant gain	Variable gain	Variable gain	Variable gain
	Attenuation Settings (dB)	31	50	20	10	10/0
	Valid Data Length	2048	2048	2048	2048	2048

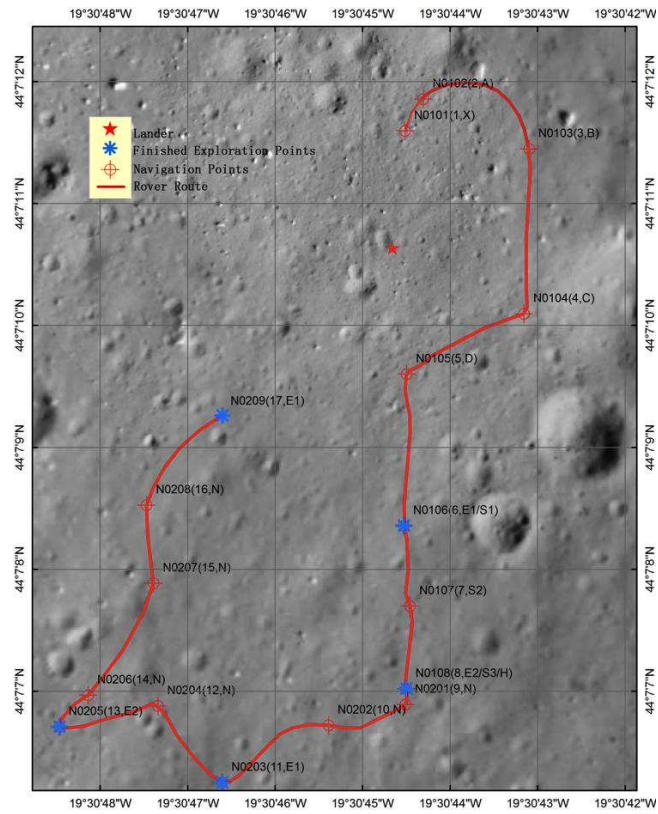


Fig. 2 The roadmap of the Yutu rover's traverse is denoted by the red line. The red star represents the CE-3 lander's landing location, the blue asterisks are the scientific exploration points and the red circles with plus signs are the navigation points. The background topographic picture was taken by a descending camera attached to the lander as it descended. The picture has a resolution of 10 cm.

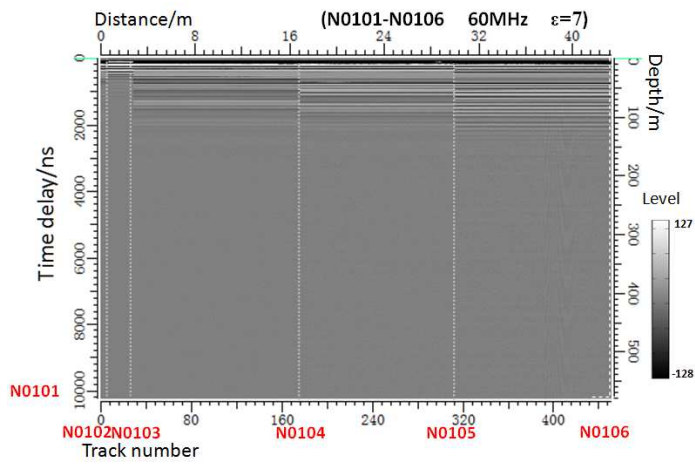


Fig. 3 A radar map of the LPR tests from points N0101 to N0106 with different parameter settings used for channel 1. The relative dielectric constant is set to be 7. This shows that different parameter settings result in different mantling layers with different detection depths.

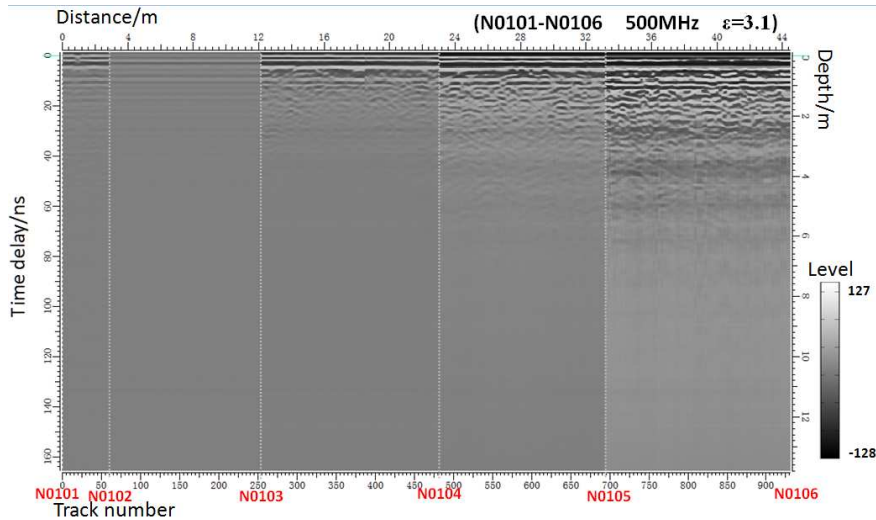


Fig. 4 The radar map of the LPR tests from points N0101 to N0106 with different parameter settings used by channel 2. The relative dielectric constant is set to be 3.1. This shows that optimal parameter settings result in good mantling layers with deeper detection depths.

One set of parameters from the points N0105 to N0106 is optimal, so the results display detailed structures in deeper regions. The parameter settings during LPR's subsequent traverse are almost same as the optimal settings but slightly different according to the actual detection. All the parameter settings are stored in the PDS index of every track radar data. Unfortunately the Yutu rover suffered major problems near the end of the second lunar day and it could not traverse anymore. Thus the radar data from points N0208 to N0209 are lost and only repeated data at the location of point N0209 could be obtained.

3 DATA PROCESSING

The scientific data are archived and distributed by National Astronomical Observatories, Chinese Academy of Sciences. Data processing has been done in order to eliminate the effect of the instrument. The radar data are divided into three levels including Level 0, Level 1 and Level 2, as shown in Table 2.

- (1) Raw data: Raw data are collected by the 50 m radio telescope in Beijing and the 40 m radio telescope in Kunming. Each station transmits the raw data by a dedicated fiber to the headquarters

Table 2 Description of Data Levels in Data Processing

Data Levels	Description of data processing
Level 0	The raw data
Level 1	Convert the unsigned numbers to signed numbers
Level 2	Level 2A: Normalization, elimination of variable gain and the effect of instrument drift Level 2B: Include the navigation point position of the Yutu rover Level 2C: Filtering

of the science and application center for lunar and deep space exploration located at National Astronomical Observatories in Beijing.

- (2) Level 1 data: The unsigned 16-bit numbers are converted to signed numbers according to their cumulative number, as defined in Equation (1).

$$X_{(m)} = S_{(m)} - 128 \times (A + 1), \quad (1)$$

where m is the index of the sampled points, $X_{(m)}$ is a 16-bit signed integer, $S_{(m)}$ is a 16-bit unsigned integer and A is the cumulative number.

- (3) Level 2 data: Based on Level 1 data, Level 2 data are divided into Levels 2A, 2B and 2C with further processing that involves normalization, geometric correction, etc.
- (a) Level 2A data: Firstly, normalize the Level 1 data between -128 and 128 . Secondly, eliminate the effect of variable gain based on the test results on the Earth before the LPR instrument was installed on the Yutu rover, thus amplitude of the relative echo signal can be calculated. In addition, we remove the DC drift using the sliding window method as shown in Equation (2).

$$Y_{(n)} = y_{(n)} - \frac{1}{n_2 - n_1 + 1} \sum_{m=n_1}^{n_2} y_{(m)},$$

$$n_1 = \begin{cases} n - \frac{N-1}{2}, & n \geq \frac{N-1}{2}, \\ 0, & n < \frac{N-1}{2}, \end{cases} \quad (2)$$

$$n_2 = \begin{cases} n + \frac{N-1}{2}, & n \leq N_e - \frac{N+1}{2}, \\ N_e - 1, & n > N_e - \frac{N+1}{2}, \end{cases}$$

where $Y_{(n)}$ is the calculated value after eliminating the effect of instrument drift, $y_{(n)}$ is the calculated value after eliminating the effect of variable gain and n is the index of sampled points. N is the sliding window size; for 60 MHz track data, N equals 201, but N equals 101 for 500 MHz track data. N_e means the number of valid points in one block of track data.

- (b) Level 2B data: While the Yutu rover was maneuvering, different navigation points were set. The coordinates of the current navigation point and the relative position according to the current navigation point are recorded in Level 2B data, thus the location of the Yutu rover could be determined.
- (c) Level 2C data: A band-pass filter based on FFT filtering was designed. Parameters for the filter included a low stop-band cut-off frequency, a low pass-band cut-off frequency, high pass-band cut-off frequency and a high of 5, 10, 100, 120, and 10, 50, 950, 1000 MHz for 60 MHz and 500 MHz respectively.

4 DATA ANALYSIS AND PRELIMINARY RESULTS

Based on the Level 2C radar data and the parameter settings in the PDS index, to obtain clear radar images, coordinate transformation, data editing, background removal, the operations of smoothing and gain resetting need to be applied. Coordinate transformation is used to obtain the trajectory of the LPR. There are two coordinate systems in radar data processing. One is the coordinate system which uses the CE-3 lander's landing point as the origin (east-north-sky) where navigation points can be calculated. In the other coordinate system, the origin is the current navigation point (north-east-Earth), from which the position where LPR data are acquired can be calculated. Notably, the navigation point might be set differently for each movement of the Yutu rover. After transformation between these two coordinate systems, the working trajectory relative to the landing point can be obtained from Equation (3).

$$(X_{\text{lander}}, Y_{\text{lander}}, Z_{\text{lander}}) = (X_0, Y_0, Z_0) + (Y_{\text{NEU}}, X_{\text{NEU}}, -Z_{\text{NEU}}), \quad (3)$$

where (X_0, Y_0, Z_0) are the coordinates of the navigation point with respect to the center of the landing site and are recorded in each block of track data, $(X_{NEU}, Y_{NEU}, Z_{NEU})$ are the coordinates of the Yutu rover with respect to the center of the current navigation point in each track of data, and $(X_{lander}, Y_{lander}, Z_{lander})$ are the coordinates of the Yutu rover with respect to the center of the landing site for each track data.

As the Yutu rover does not traverse at a constant speed, frequently stopping and maneuvering, about 13% of track data are valid. A lot of tracking data were sampled when the Yutu rover was stationary. The purpose of data editing is to extract valid data from all data to obtain a uniform distribution across the lunar surface. According to the time label for movements of the Yutu rover, valid track data during the traverse of the Yutu rover are selected.

Background noise exists in the radar echo signal, and it could be removed by subtracting the mean of all the track data in a certain period from each block of track data according to Equation (4). The time period could be determined by the system parameter settings of the LRP and the actual working status of the device.

$$Y_{(n)} = y_{(n)} - \frac{1}{N} \sum_{n=1}^N y_{(n)}, \quad (4)$$

where y_n represents the original radar track data, Y_n represents radar track data after the removal of background, n denotes the sequential number for the radar track data in a certain period of time and N is the total number of radar track data in a certain period of time.

To generate an overall radar image, radar data from different periods need to be spliced together. Smoothing has been applied between data points as defined in Equation (5). By comparison, N equals 7 returns a better fit, that is, considering that the track data have a mean of 7.

$$Y_{(n)} = \frac{1}{n_2 - n_1 + 1} \sum_{i=n_1}^{n_2} y_{(i)}, \quad (5)$$

$$n_1 = \begin{cases} n - \frac{N-1}{2}, & n > \frac{N-1}{2}, \\ 1, & n \leq \frac{N-1}{2}, \end{cases}$$

$$n_2 = \begin{cases} n + \frac{N-1}{2}, & n \leq N_{\text{all}} - \frac{N+1}{2}, \\ N_{\text{all}}, & n > N_{\text{all}} - \frac{N+1}{2}, \end{cases}$$

where N_{all} means the number of the all radar track.

Gain resetting aims to amplify a weak radar signal, so we can identify layers in deeper regions. Here, non-linear gain in the area of interest is considered.

Based on analysis of the Apollo samples and other previous studies (Olhoeft & Strangway 1975; Haskin et al. 1991), in mare regions the relative dielectric constant of the regolith was measured to be in the range 2.32 to 3.49, and the relative dielectric constant of the lunar rock is in the range 6.62 to 8.76. Here we assume the relative dielectric constant to be 3.1 for the regolith and 7 for the lunar rock. According to calibration tests that were performed by the Institute of Electronics, Chinese Academy of Sciences, the time delay of the radar echo signal transmitted from the lunar surface is 69.664 ns and 28.203 ns for channel 1 and channel 2 respectively, thus the lunar surface is denoted by this value for time delay.

The initial results of the two frequency channels during the second lunar day (from 11 to 15 January 2013 UTC) are presented in the following figures. Figures 5 and 6 show the results from points N0201 to N0207.

5 DISCUSSION

Error analysis is very import but difficult work. According to the instrument's setting parameters, the length of valid data for each track is 4096 points at 60 MHz and 2048 points at 500 MHz. Using the repeated raw data at one point where data were taken when the Yutu rover was stationary, the

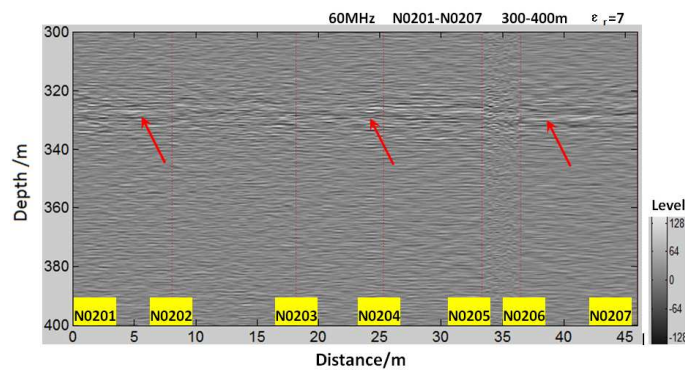


Fig. 5 The radar result of 60 MHz from N201 to N207. The depth range for the plot is from 300 m to 355 m. The arrows indicate the existence of prominent reflectors at a depth of about 330 m with the assumption that the basalt has a relative dielectric constant of 7.

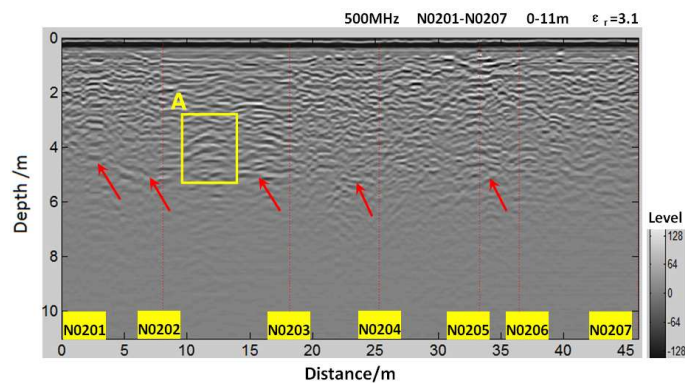


Fig. 6 The stratification of regolith along the Yutu rover's transverse path with the assumption that the regolith has a relative dielectric constant of 3.1. The arrows indicate the layer in the regolith where the thickness of the regolith is 4–6 m. The region labeled by A has a typical hyperbolic shape that might be caused by a rock underneath the regolith.

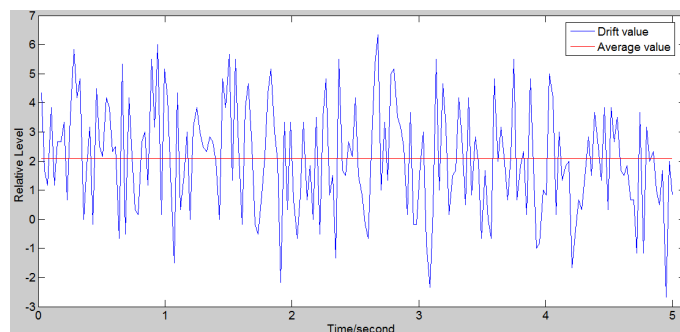


Fig. 7 The instrument drift at sample point 1000 in one block of track data observed at the location point N0209 in 5 min (60 MHz). The average is 2.1, and the standard deviation is 1.9, so the possible interval of the amplitude with a 95% confidence level is 2.1 ± 3.8 .

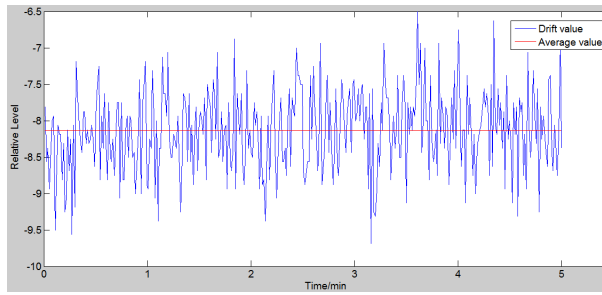


Fig. 8 The instrument drift at sample point 1000 in one block of track data observed at the location point N0209 in 5 min (500 MHz). The average is -8.1 , and the standard deviation is 0.4 , so the possible interval of the amplitude with a 95% confidence level is -8.1 ± 0.8 .

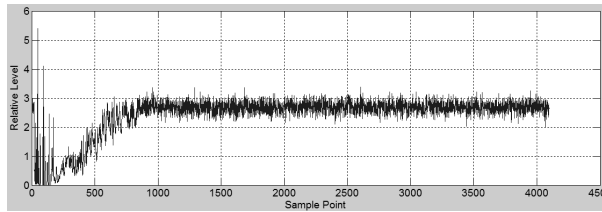


Fig. 9 The instrument standard deviation at 60 MHz. The average standard deviation is 2.4 . The standard deviation is relatively large in less than 250 points since the radar echo signals are strong in the shallow region. From point 250 to point 900, the standard deviation is smaller because the receiving system is in a state of nonlinear saturation. The standard deviation is stabilized afterwards.

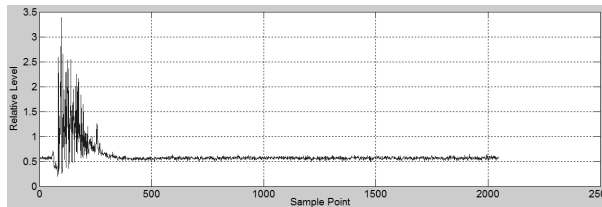


Fig. 10 The instrument standard deviation at 500 MHz. The average standard deviation is 0.6 . The standard deviation is relatively large in less than 250 points because the radar echo signals are strong in the shallow region. The standard deviation is stabilized afterwards.

system drift is calculated and shown in Figures 7 and 8. Also, the system standard deviations using all the repeated raw data at all points where data were taken are analyzed. Figures 9 and 10 show the standard deviation for each sample point, and the average system standard deviations are 2.4 and 0.6 at 60 MHz and 500 MHz respectively.

6 CONCLUSIONS

Mare Imbrium is the largest impact basin on the nearside of the Moon and the formation age of Imbrium is 3.85 Gyr (Wilhelms et al. 1987). Between 2.01 and 3.57 Gyr, when mare basalts were

erupting, older basalts could have been covered by younger basalts (Hiesinger et al. 2000; Hiesinger et al. 2010). The radar sounder carried by Apollo 17 indicates that there are two continuous buried horizontal layers in Mare Serenitatis. One layer is at a depth of about 0.9 km and the other is at about 1.6 km (Peeples et al. 1978). The radar sounder onboard the KAGUYA spacecraft also revealed that there is a two-layer structure in Mare Imbrium and the apparent depths are 320–550 m and 920–1050 m respectively (Ono et al. 2009, 2010). Apparent depth is defined as the penetrating depth with $\varepsilon_r = 1$. The LPR observations also reveal that Mare Imbrium has subsurface stratifications.

Figure 5 very clearly indicates the presence of one prominent reflector at depths of hundreds of meters. Apparent depth with $\varepsilon_r = 1$ is assumed to be 873 m, and the corresponding layer is estimated to have a depth of about 330 m considering $\varepsilon_r = 7$. The buried regolith layer might have been accumulated during the depositional hiatus of mare basalts.

The regolith on the Moon's surface is a highly comminuted surface layer, which was formed by billions of years of collisions. The regolith is not uniform and structures with multiple layers have been observed, as shown in Figure 6. Observations with the LPR show the regolith around the landing place in Mare Imbrium is about 4–6 m deep. Also, the typical hyperbolic radar echo signal recorded in the A region might indicate that a rock lies underneath the regolith.

Since the Yutu rover had severe problems during its second lunar day, it is pity that the Yutu rover only transversed a limited distance. Nevertheless, the LPR worked successfully and performed the first on site exploration of structure under the lunar subsurface. In total, 566 MB of data were obtained. The preliminary results have been derived, and further analysis will be carried out.

Acknowledgements We thank Neil Roddis for great help with English correction. This work was supported by the National Natural Science Foundation of China (Grant Nos. 11173038 and 11203046). We also thank the Lunar and Deep Space Exploration Department, National Astronomical Observatories, Chinese Academy of Sciences (NAOC) for providing the radar data.

References

- Fang, G.-Y., Zhou, B., Ji, Y.-C., et al. 2014, *RAA (Research in Astronomy and Astrophysics)*, 14, 1607
- Haskin, L., Warren, P., Heiken, G. H., Vaniman, D. T., & French, B. M. 1991, *CUP*, 447
- Hensley, S., Gurrola, E., Harcke, L., et al. 2011, in *Lunar and Planetary Science Conference*, 42, 1813
- Hiesinger, H., Head, J., Wolf, U., Jaumann, R., & Neukum, G. 2010, *Journal of Geophysical Research: Planets* (1991–2012), 115
- Hiesinger, H., Jaumann, R., Neukum, G., & Head, J. W. 2000, *J. Geophys. Res.*, 105, 29239
- Ip, W.-H., Yan, J., Li, C.-L., & Ouyang, Z.-Y., 2014, *RAA (Research in Astronomy and Astrophysics)*, 14, 1511
- Kirk, R., Cook, D., Howington-Kraus, E., et al. 2010, in *A Special Joint Symposium of ISPRS Technical Commission IV & AutoCarto in Conjunction with ASPRS/CaGIS 2010 Fall Specialty Conference*
- Olhoeft, G. R., & Strangway, D. W. 1975, *Earth and Planetary Science Letters*, 24, 394
- Ono, T., Kumamoto, A., Kasahara, Y., et al. 2010, *Space Sci. Rev.*, 154, 145
- Ono, T., Kumamoto, A., Nakagawa, H., et al. 2009, *Science*, 323, 909
- Peeples, W. J., Sill, W. R., May, T. W., et al. 1978, *J. Geophys. Res.*, 83, 3459
- Shkuratov, Y. G., & Bondarenko, N. V. 2001, *Icarus*, 149, 329
- Shkuratov, Y. G., Kaydash, V. G., & Opanasenko, N. V. 1999, *Icarus*, 137, 222
- Spudis, P., Bussey, D., Baloga, S., et al. 2010, *Geophysical Research Letters*, 37
- Thompson, T. W. 1987, *Earth Moon and Planets*, 37, 59
- Thompson, T. W., & Dyce, R. B. 1966, *J. Geophys. Res.*, 71, 4843
- Wilhelms, D. E., McCauley, J. F., & Trask, N. J. 1987, *The Geologic History of the Moon* (Washington: U.S. G.P.O.)
- Yamaji, A. 1998, *Mem. Geol. Soc. Japan.*, 50, 213